Structural, Magnetic and Dielectric Studies of $Pb_{0.9}Bi_{0.1}Fe_{0.55}Nb_{0.45}O_3$ Multiferroic Solid solution

S T Dadami[1], S Matteppanavar[1], I Shivaraja[1], S Rayaprol[2], B Angadi[1,*]

[1]Department of Physics, JB Campus, Bangalore University, Bangalore – 560056 INDIA
[2]UGC-DAE-Consortium for Scientific Research, Mumbai Centre, BARC Campus, Mumbai – 400085 INDIA

[*]Corresponding author:brangadi@gmail.com

Abstract. Single phase $Pb_{0.9}Bi_{0.1}Fe_{0.55}Nb_{0.45}O_3$ (PFN-BFO) multiferroic solid solution was synthesized through single step solid state reaction method using low temperature annealing technique. The crystal structure, microstructure, magnetic and dielectric properties of PFN-BFO solid solution were investigated at room temperature (RT). Sintered samples were then subjected to XRD analysis and it revealed the formation of single phase without any impurities. The structural analysis was carried out by Rietveld Refinement technique through the Full Prof suite. The RT Rietveld refined XRD pattern confirms the monoclinic structure with *Cm* space group and obtained cell parameters are a = 5.666(3)Å, b = 5.667(4)Å, c = 4.017(2)Å and β = 89.943(4)º. The surface morphology of the sample was studied by Scanning electron microscope (SEM) and average grain size was estimated to be ~5µm. M-H curve shows the weak ferromagnetic kind of behaviour with antiferromagnetic ordering. Room temperature dielectric constant, loss tangent and impedance spectroscopic data were measured at different frequencies (100Hz - 5MHz). The impedance spectroscopy reveals the contribution from the grains towards the electrical parameters.

Keywords: Multiferroic, Solid State Reaction, X-ray diffraction, Magnetic, Dielectrics.

1. Introduction

Multiferroic materials that exhibit more than one ferroic orders in the same phase have attracted much attention in recent years due to their potential applications in multifunctional devices. There exists a coupling between the ferromagnetic and ferroelectric orders, known as magnetoelectric (ME) coupling and this coupling is used in various practical devices such a multifunctional sensors, actuators, data storage, broadband magnetic field sensors, microwave phase shifters and magnetoelectric memory cells [1]. There are very few single phase materials in nature which exhibit ferroelectric and ferromagnetic properties simultaneously. Among them, $PbFe_{0.5}Nb_{0.5}O_3$ (PFN) and $BiFeO_3$ (BFO) are exhibiting their multiferroicity below and above room temperature, respectively. At room temperature PFN has a monoclinic structure with *Cm* space group. PFN is considered to be antiferromagnetically ordered below its Néel temperature (T_N ~155K) and it undergoes transition from paraelectric (PE) to ferroelectric (FE) phase at Curie temperature (T_C~ 385K) [2, 3], due to the structural transition from Centro-symmetric (cubic) to non-centrosymmetric (monoclinic phase) structure. In addition to ferroelectric and antiferromagnetic features, the magneto electric (ME) coupling observed below T_N (below RT) offers significant interest in PFN for potential applications as well as for fundamental understanding. Another well-known multiferroic material is $BiFeO_3$ (BFO) which exhibits ferroelectric (T_C =1103K) and antiferromagnetic (T_N = 643K) orderings above RT [4].

At room temperature it has a rhombohedral structure with *R3c* space group. It also exhibits a very weak magneto-electric coupling. It is known in the literature that the synthesis of single phase PFN and BFO with perovskite structure has been difficult by the conventional methods, due to the formation of unwanted pyrochlore ($Pb_2Nb_2O_7$, $Pb_2Nb_2O_5$, $Bi_2Fe_4O_9$ and $Bi_{46}Fe_2O_{72}$) [4, 5] or other secondary phases at higher temperatures.

In this present work, we employed single-step calcination and a low temperature sintering technique to achieve single phase $Pb_{0.9}Bi_{0.1}Fe_{0.55}Nb_{0.45}O_3$ (PFN-BFO) solid solution. Detailed structural, magnetic and dielectric studies were carried out at RT through XRD, SEM, M-H, Dielectric constant and loss tangent measurements.

2. Experimental

The single phase PFN-BFO was synthesized through the single step solid state reaction method [6] using the stoichiometric amounts of reagent grade $Pb(NO_3)_2$, Bi_2O_3, Fe_2O_3 and Nb_2O_5 precursors. $Pb(NO_3)_2$ and Bi_2O_3 were added 1% extra in order to maintain the loss due to evaporation during annealing. They were ground in an ethanol medium for 2 hr. Calcination was done at 700 °C for 2 hr make the homogenous mixture. The calcined powder was ground with 5% polyvinyl alcohol (PVA) as a binder. The 10 mm diameter and 2 to 3 mm thick pellets were uniaxially pressed at 50 kN using a hydraulic press and sintered at an optimized temperature of 800 °C for 3 hr in a closed Pb and Bi rich environment to minimize the PbO and Bi_2O_3 evaporation. PFN-BFO samples were characterized with the powder XRD using Phillips (1070 model) diffractometer with Cu Kα (1.5406 Å) radiation for the phase formation. The structural analysis was carried out using FullProf program. The magnetic measurements were carried out using a vibrating sample magnetometer (VSM). The Dielectric constant, the loss tangent as a function of frequency and the impedance spectroscopy were analysed at RT.

3. Results and Discussions

3.1. Structural Studies

Figure 1 shows the XRD pattern of single phase PFN-BFO solid solution and is matching well with the JCPDS pattern no. 89-8043. Various calcination and sintering temperature and time duration were carried out to achieve single phase and it is found that at 700 °C for 2 hr calcination and at 800 °C for 3 hr sintering are the optimum conditions. Rietveld refinement was carried out on RT XRD and it confirms the monoclinic structure with the *Cm* space group. The obtained structural parameters from XRD data are a = 5.666(3) Å, b = 5.667(4) Å, c = 4.017(2) Å and β = 89.943(4) ° and α = 90°, β = 89.943(4)°, γ = 90°. R-factors are R_P = 15.7; R_{WP} = 20.7; R_{Exp} = 16.72; χ^2 = 1.54. Figure 2 shows the scanning electron microscopy (SEM) micrograph of PFN-BFO solid solution showing an average grain size of ~ 5 μ m with uniform morphology.

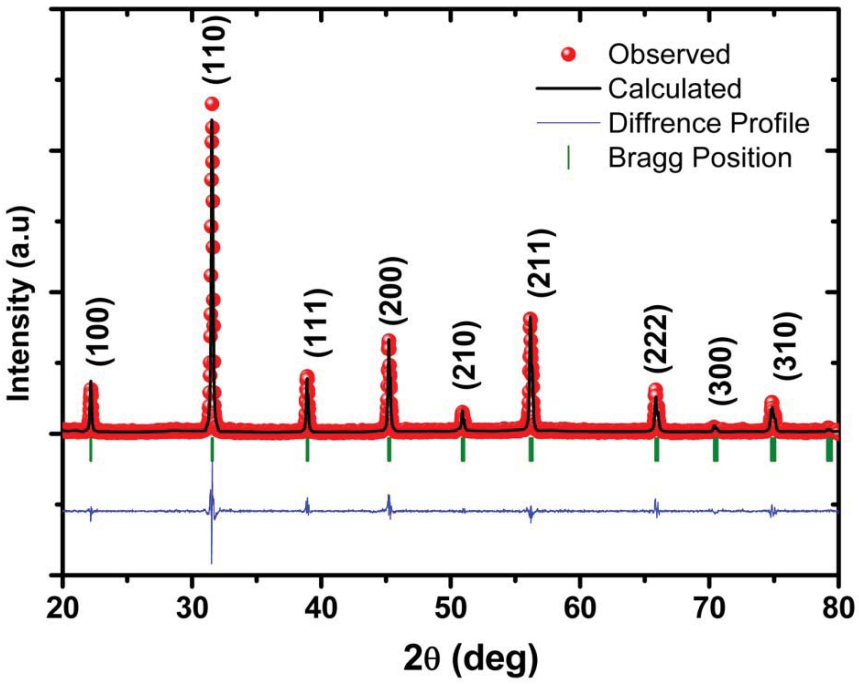

Figure 1 RT Rietveld refined X-ray diffraction pattern of PFN-BFO. Observed (red circle) and calculated (continuous black line) profiles of XRD are shown for PFN-BFO. The lowest curve (blue line) shows the difference between experimental and calculated patterns.

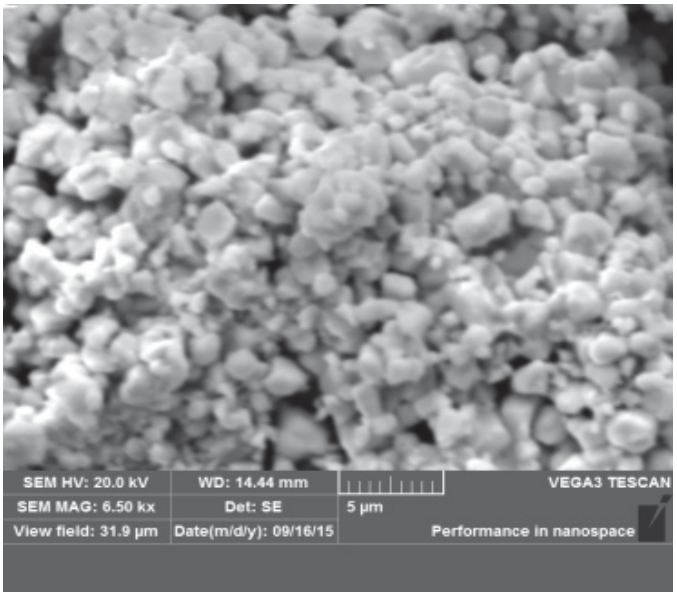

Figure 2 Scanning Electron Micrograph of PFN-BFO solid solution.

3.2. Magnetic Studies

Figure 3 show the magnetization as a function of field measured at RT. The slim M - H loop with small opening of hysteresis loop gives a clear signature of existence of weak ferromagnetic behaviour. The magnetic order is mainly due to a super exchange interaction mechanism occurring between the Fe – O – Fe or O – Fe – O [5]. Inset shows zoomed view of M - H loop. The remnant (M_r) and coercive field (H_c) are found to be 2.4081E-03 emu /g and 26.539 Gauss respectively.

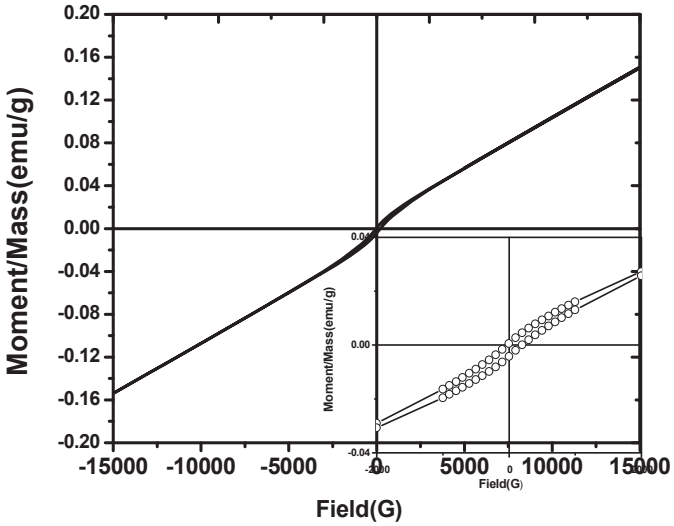

Figure 3 M - H loop of PFN-BFO solid solution at RT

3.3. Dielectric Studies

Figure 4 shows the dielectric constant (ε') and loss tangent ($\tan(\delta)$) of the sintered pellet of the PFN - BFO sample have been measured as a function of frequency (100 Hz- 5MHz) at RT. The dielectric constant decreases with increasing frequency. At higher frequency dielectric constant drops to rather low value. Such a drastic decrease in dielectric constant with frequency can be explained in terms of model based on barrier layer formation. The formation of barrier layers at the grain and grain boundary interfaces give rise to interfacial space charge polarization. Interfacial polarizability results due to the difference in the conductivity of the grains and the grain boundaries. So the Maxwell-Wagner type dielectric relaxation results due to the separation of grains by more insulating grain boundary. Generally in perovskite materials loss of oxygen occurs during sintering at higher temperature. This creates the Fe^{2+} and oxygen vacancies which increase the electrical conduction, dielectric loss and space charge accumulation at the grain boundaries.

The dielectric loss is high at lower frequencies and decreases as the frequency increases. At lower frequencies the resistance imposed by the grain boundaries is more and hence the loss is more. At higher frequencies the periodic reversal of the electric field occurs so fast that there is no excess of charge diffusion in the direction of the applied field. So, the charge accumulation decreases, leading to a decrease in the value of the dielectric loss. A peak in the dielectric loss occurs when $\omega\tau = 1$, i.e. when the relaxation frequency synchronises with the applied frequency.

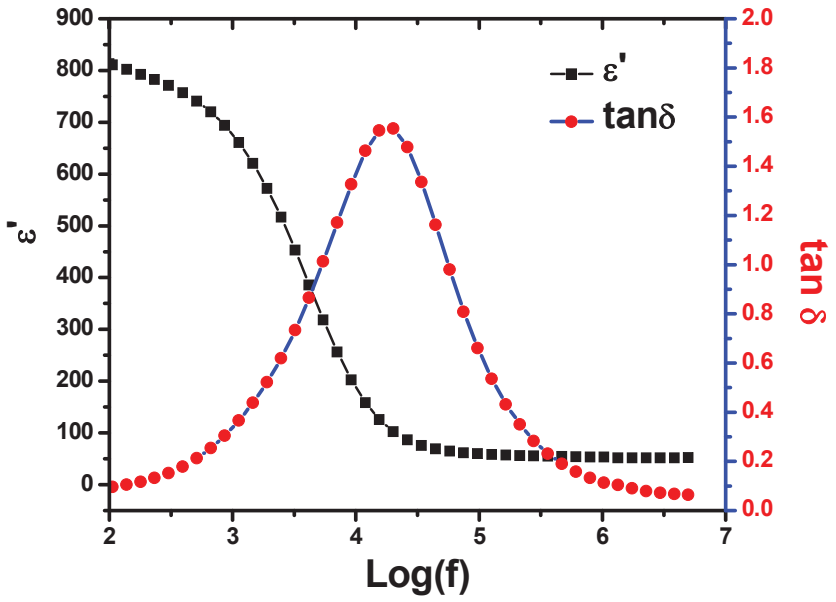

Figure 4 Dielectric constant (ε' and tan δ) vs. frequency for PFN - BFO solid solution at RT.

3.4. Complex Impedance Studies

Impedance measurement is widely used for the electrical characterization of ceramic materials [7, 8, 9] over a wide range of frequency. The grain, grain boundary and material electrode contributions towards the electrical properties are easily separated by this technique. The electrical response of the material can be studied by using the basic formalisms via the complex permittivity (ε*), complex impedance (Z^*), complex admittance(Y^*), complex electric modulus (M*) and dielectric loss or dissipation factor (tan δ) which are interrelated to each other. The following formalisms of impedance spectroscopy have been used to study the frequency dependence of electrical properties of the material.

Complex permittivity,

$$\varepsilon^*(\omega) = \varepsilon' - j\varepsilon'' \qquad (1)$$

ε' is the real part and ε'' is the imaginary part of the permittivity. The first term is the contribution of the energy storage and second term is due to energy loss.

Complex impedance

$$Z^*(\omega) = Z' - Z'' \qquad (2)$$

Z' and Z'' are the real and imaginary part of the impedance and are given by

$$Z' = |Z|\cos(\delta) \quad \text{and} \quad Z'' = |Z|\sin(\delta) \tag{3}$$

And the loss tangent,

$$\tan(\delta) = \frac{Z'}{Z''} \tag{4}$$

Figure 5 shows the complex impedance spectra (Z'' vs. Z') of PFN-BFO sample at room temperature. For a Debye type of relaxation, a perfect semicircle is observed (with its centre on Z' axis). But the Figure 5 shows depressed single semicircle whose centre is found below Z' axis, suggests a deviation from the ideal Debye type behaviour and confirms the presence of bulk contribution only. Inset Figure 5 shows the zoomed view of the Cole Cole plot and it clearly shows the formation of a single semicircle.

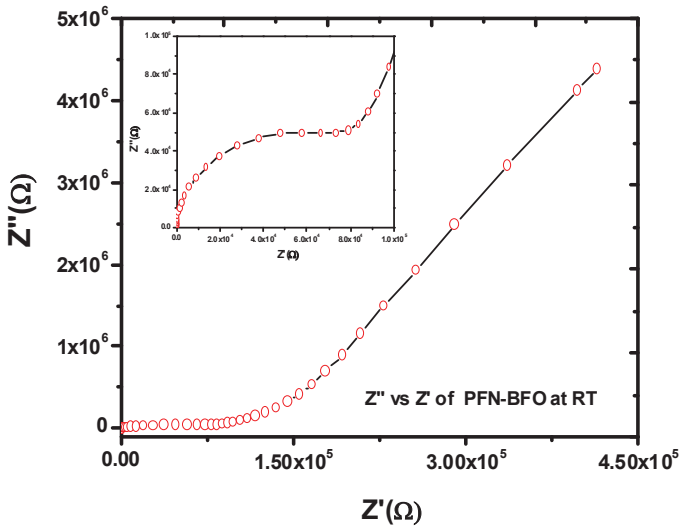

Figure 5 Z'' vs. Z' of PFN-BFO ceramic at RT.

4. Conclusion

The PFN-BFO solid solution was synthesized by single step solid state reaction method using lower calcination (700 °C /2hr) and sintering (800 °C /3hr). The 100% perovskite phase with no traces of pyrochlore phase was obtained. The refined XRD data confirms the monoclinic structure with the *Cm* space group. Scanning electron microscopy (SEM) micrograph shows an average grain size of ~ 5 μ m with uniform morphology. RT M-H loop confirms the weak ferromagnetic ordering. Dielectric constant shows a larger dispersion at lower frequencies and loss tangent shows relaxation behaviour. The RT impedance spectroscopy shows a single semicircle and is depressed, showing the departure from ideal Debye type of behaviour. Also the single semicircle reveals the contributions from the grains towards the electrical parameters.

Acknowledgements

The author Sunanda Dadami is grateful to University Grants Commission (UGC) Government of India, for the award of UGC- FDP fellowship to carry out this work. Authors (SM, SI and BA) are grateful to UGC DAE CSR Mumbai centre for providing experimental facilities and student fellowship in CRS-M-159 and CRS-M-200 projects. Also authors thank Prof. R. N. Bhowmik, Department of Physics, Pondicherry University, Pondicherry for providing VSM measurement facility.

References

[1] Wang Y P, Yuan G L, Chen X Y, Liu J M and Liu Z G. 2006 *J. Phys. D: Appl. Phys*. **39** 2019.
[2] Matteppanavar S, Angadi B and Rayaprol S 2014 *Physica B* **448** 229.
[3] Matteppanavar S, Rayaprol S, Singh K, Reddy V R and Angadi B 2015 *J. Mater. Sci.* **50** 4980.
[4] Singh S P, Pandey D, Yoon S, Baik S and Shin N 2007 Appl. Phys. Lett. **90** 242915.
[5] Matteppanavar S, Rayaprol S, Anupma A V, Angadi B and Sahoo B, 2015 *Cerm. International* **41** 11680.
[6] Dadami S T , Matteppanavar S, Shivaraja I, Rayaprol S, Angadi B, Sahoo B, 2016 http://dx.doi.org/10.1016/j. jmmm.2016.01.092i.
[7]Yang Y, Liu J M, Huang H B, Zou W Q, Bao P and Liu Z G, 2004 *Phys. Rev. B* **70** 132101.
[8] Kumar N, Patil S K and Choudary R N P 2014 *J. Aloys Comp*., **615** 456.
[9] Lanfredi S and Rodriguez A C M 1999 *J. Appl. Phys*., **86** 2215.